

Multiple Parton Interactions, top–antitop and $W + 4j$ production at the LHC

Ezio Maina^{a,b}

^a *INFN, Sezione di Torino, Italy,*

^b *Dipartimento di Fisica Teorica, Università di Torino, Italy*

ABSTRACT: The expected rate for Multiple Parton Interactions (MPI) at the LHC is large. This requires an estimate of their impact on all measurement foreseen at the LHC while opening unprecedented opportunities for a detailed study of these phenomena. In this paper we examine the MPI background to top–antitop production, in the semileptonic channel, in the early phase of data taking when the full power of b -tagging will not be available. The MPI background turns out to be small but non negligible, of the order of 20% of the background provided by $W + 4j$ production through a Single Parton Interaction. We then analyze the possibility of studying Multiple Parton Interactions in the $W + 4j$ channel, a far more complicated setting than the reactions examined at lower energies. The MPI contribution turns out to be dominated by final states with two energetic jets which balance in transverse momentum, and it appears possible, thanks to the good angular resolution of ATLAS and CMS, to separate the Multiple Parton Interactions contribution from Single Parton Interaction processes. The large cross section for two jet production suggests that also Triple Parton Interactions (TPI) could provide a non negligible contribution. Our preliminary analysis suggests that it might be indeed possible to investigate TPI at the LHC.

Contents

1. Introduction	1
2. Calculation	2
3. MPI background to top pair production	6
4. Studying MPI in $W + 4j$ processes	9
5. Conclusions	13

1. Introduction

The presence of Multiple Parton Interactions (MPI) in high energy hadron collisions has been convincingly demonstrated [1, 2].

MPI rates at the LHC are expected to be large, making it necessary to estimate their contribution to the background of interesting physics reactions. Previous studies evaluated the MPI background to Higgs production in the channel $pp \rightarrow WH \rightarrow l\nu b\bar{b}$, [3], $4b$ production [4] and WH, ZH production [5]. On the other hand, their abundance at the LHC makes it possible to study MPI experimentally in details, testing and validating the models which are used in the Monte Carlo's [6, 7, 8, 9] to describe these important features of hadron scattering. It is therefore of interest to search for new reactions in which MPI can be probed and to study in which kinematical regimes they are best investigated. Different reactions involve different combinations of initial state partons, for instance $\gamma + 3j$, $Z + 3j$, $W + 3j$ and $4j$ MPI processes test specific sets of quark and gluon distributions inside the proton. The comparison of several MPI processes will also allow to study the possible x -dependence of these phenomena, namely the dependence on the fraction of momentum carried by the partons.

CDF found no evidence of x -dependence in their data which included jets of transverse momentum as low as five GeV. However in Ref.[10, 11, 12] it was shown that correlations between the value of the double distribution functions for different values of the two momentum fractions x_1, x_2 are to be expected, even under the assumption of no correlation at some scale μ_0 , as a consequence of the evolution of the distribution functions to a different scale μ , which is determined by an equation analogous to the usual DGLAP equation. In [12] the corrections to the factorized form for the double distribution functions have been estimated. They depend on the factorization scale, being larger at larger scales Q , and on the x range, again being more important at larger momentum fractions. For $Q = M_W$ and $x \sim 0.1$ the corrections are about 35% for the gluon-gluon case. Moreover Ref.[12] showed that the correlations in x_1, x_2 space are different for different pairs of partons, pointing to an unavoidable flavour dependence of the double distribution functions.

In this paper we examine

- the background generated by MPI to $t\bar{t}$ production particularly in the early phase of data taking at the LHC in which b -tagging might perform poorly or not at all;
- the possibility of studying MPI in the $W + 4j$ channel.

In all cases we assume that one W decays leptonically, allowing for easy triggering.

The LHC will be a top-antitop factory and the large rate will allow accurate measurements of the top mass and cross section. The top mass is one the most crucial ingredients in the high precision global fit of the Standard Model and together with the information provided by the Higgs searches will allow very stringent tests of the SM. With its five final state particles, $W + 4j$ production gives the opportunity to study MPI in a more complex setting than in previous analyses which have typically involved a combination of two $2 \rightarrow 2$ processes.

The large expected cross section for two jet production suggests that also Triple Parton Interactions (TPI) could provide a non negligible contribution¹. If this were the case, it would open the exciting possibility of probing TPI, on which we have essentially no information so far.

In Sect. 2 the main features of the calculation are discussed. Then we present our results in Sect. 3 and Sect. 4. Finally we summarize the main points of our discussion.

2. Calculation

If no b -tagging is assumed the MPI processes which provide a background to $t\bar{t}$ and more generally contribute to $Wjjjj$ through Double Parton Interactions (DPI) are

- $jj \otimes jjW$
- $jjj \otimes jW$
- $jjjj \otimes W$

where the symbol \otimes stands for the combination of one event for each of the two final states it connects.

The cross section for DPI has been estimated as

$$\sigma = \sigma_1 \cdot \sigma_2 / \sigma_{eff} \quad (2.1)$$

where σ_1, σ_2 are the cross sections of the two contributing reactions. The customary symmetry factor, which is equal to two if the two reactions are indistinguishable and equal to one when they are different is always one in the present case. We have used $\sigma_{eff} = 14.5$ mb as measured by CDF [2] at the Tevatron. In Ref.[13] Treleani argues that a more appropriate value at $\sqrt{s} = 1.8$ TeV is 10 mb which translates at the LHC into $\sigma_{eff}^{LHC} = 12$ mb. Since σ_{eff} appears as an overall factor in our results it is easy to take into account the smaller value advocated in [13].

The only TPI process contributing to $Wjjjj$ is

¹This issue was raised by the referee, whose role we gratefully acknowledge.

- $jj \otimes jj \otimes W$.

It is worth mentioning that this is probably the simplest process and the one with the largest rate which can give access to Triple Parton Interactions at the LHC, since it involves two instances of two jet production and a Drell-Yan interaction which allows to separate this kind of events from the multiple jet background generated by QCD.

The cross section for TPI, under the same hypotheses which lead to Eq.(2.1), can be expressed as:

$$\sigma = \sigma_1 \cdot \sigma_2 \cdot \sigma_3 / (\sigma'_{eff})^2 / k \quad (2.2)$$

where k is a symmetry factor. σ'_{eff} has not been measured, and in principle it could be different from σ_{eff} . However, in the absence of actual data, we will assume $\sigma'_{eff} = \sigma_{eff}$ and since two of the reactions in Eq.(2.2) are indistinguishable we will take $k = 2$. In the following we will keep the TPI contribution, which is affected by larger uncertainties, separated from the DPI predictions which are based on firmer ground.

Three perturbative orders contribute to $4j + \ell\nu$ at the LHC through Single Parton Interactions. The $\mathcal{O}(\alpha_{EM}^6)$ and $\mathcal{O}(\alpha_{EM}^4 \alpha_S^2)$ samples have been generated with PHANTOM [14, 15, 16], while the $\mathcal{O}(\alpha_{EM}^2 \alpha_S^4)$ sample has been produced with MADEVENT [17]. All reactions contributing to MPI have been generated with MADEVENT. Both programs generate events in the Les Houches Accord File Format [18]. In all samples full matrix elements, without any production times decay approximation, have been used.

The $\mathcal{O}(\alpha_{EM}^4 \alpha_S^2)$ contribution is dominated by $t\bar{t}$ production. It includes the two main mechanism which yield top-antitop pairs, that is $gg \rightarrow t\bar{t}$ and $q\bar{q} \rightarrow t\bar{t}$. A small, purely electroweak contribution to $q\bar{q} \rightarrow t\bar{t}$ processes is included in the $\mathcal{O}(\alpha_{EM}^6)$ event set.

All samples have been generated with the following cuts:

$$\begin{aligned} p_{T_j} &\geq 30 \text{ GeV}, \quad |\eta_j| \leq 5.0, \\ p_{T_\ell} &\geq 20 \text{ GeV}, \quad |\eta_\ell| \leq 3.0, \\ M_{jj} &\geq 60 \text{ GeV} \end{aligned} \quad (2.3)$$

where $j = u, \bar{u}, d, \bar{d}, s, \bar{s}, c, \bar{c}, b, \bar{b}, g$.

The relatively high p_{T_j} threshold ensures that the processes we are interested in can be described by perturbative QCD and that our results will not be sensitive to the details of the low p_T underlying event.

We have taken $M_t = 175 \text{ GeV}$.

The cross sections for the reactions which enter the MPI sample are shown in Tab.1 and Tab.2 for DPI and TPI respectively. We have combined at random one event from each of the reactions which together produce the $jjjj(\mu^- \bar{\nu}_\mu + \mu^+ \nu_\mu)$ final state through MPI, and have required that each pair of colored partons in the final state satisfy $M_{jj} \geq 60 \text{ GeV}$. This implies that the combined cross section corresponds to the product of the separate cross sections divided by the appropriate power of σ_{eff} only for the $jjjj \otimes W$ case. In all other cases there is a reduction due to the requirement of a minimum invariant mass for all jet pairs since additional pairs are formed when the two events are superimposed. The

Process	Cross section	Combined
$j\bar{j}$	1.44e8 pb	4.03 pb
$j\bar{j}(\mu^-\bar{\nu}_\mu + \mu^+\nu_\mu)$	6.54e2 pb	
$j\bar{j}\bar{j}$	7.64e6 pb	0.68 pb
$j(\mu^-\bar{\nu}_\mu + \mu^+\nu_\mu)$	1.82e3 pb	
$j\bar{j}\bar{j}\bar{j}$	1.16e6 pb	0.88 pb
$\mu^-\bar{\nu}_\mu + \mu^+\nu_\mu$	1.09e4 pb	

Table 1: Cross sections for the processes which contribute to $4j + \ell\nu$ through DPI. The selection cuts are given in Eq.(2.3). Notice that the combined cross section corresponds to $\sigma_1 \cdot \sigma_2 / \sigma_{eff}$ only for the $j\bar{j}\bar{j}\bar{j} \otimes W$ case. In all other cases there is a reduction due to the requirement of a minimum invariant mass for all jet pairs since additional pairs are formed when the two events are superimposed.

Process	Cross section	Combined
$j\bar{j}$	1.44e8 pb	0.27 pb
$j\bar{j}$	1.44e8 pb	
$\mu^-\bar{\nu}_\mu + \mu^+\nu_\mu$	1.09e4 pb	

Table 2: Cross sections for the processes which contribute to $4j + \ell\nu$ through TPI. The selection cuts are given in Eq.(2.3).

largest contribution is given by processes in which the W boson is produced in association with two jets in one interaction and the other two jets are produced in the second one. As a consequence, as in the case of $\gamma + 3j$ studied by CDF [2] most of the events contain a pair of energetic jets with balancing transverse momentum. The next largest contribution is due to Drell-Yan processes combined with four jet events. The smallest, but still sizable, DPI contribution is given by processes in which the W boson is produced in association with one jet, which balances the W transverse momentum, and the other three jets are produced in the second interaction. The cross section for TPI is 0.27 pb, about 5% of all MPI processes.

We work at parton level with no showering and hadronization. Color correlations between the two scatterings have been ignored. They are known to be important at particle level [19] but are totally irrelevant at the generator level we are considering in this paper. The two jets with the largest and smallest rapidity are identified as forward and backward jet respectively. The two intermediate jets will be referred to as central jets in the following.

The neutrino momentum is reconstructed according to the usual prescription, requiring the invariant mass of the $\ell\nu$ pair to be equal to the W boson nominal mass,

$$(p^\ell + p^\nu)^2 = M_W^2, \quad (2.4)$$

in order to determine the longitudinal component of the neutrino momentum. This equa-

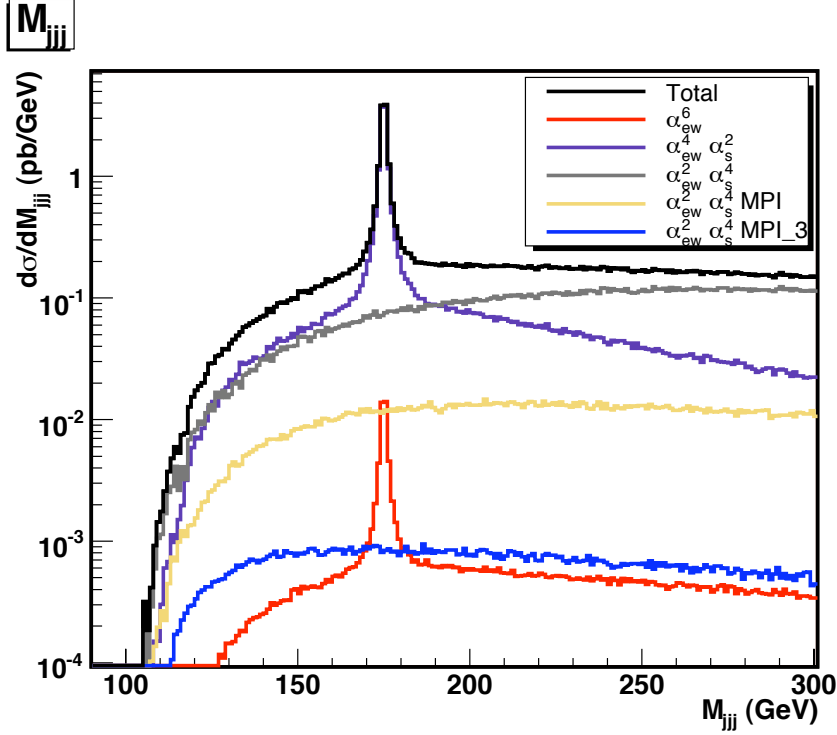


Figure 1:

M_{jjj} distribution for the different contributions and for their sum. Cuts as in Eq.(2.3) and Eq.(3.1).

tion has two solutions,

$$p_z^\nu = \frac{\alpha p_z^\ell \pm \sqrt{\alpha^2 p_z^{\ell 2} - (E^{\ell 2} - p_z^{\ell 2})(E^{\ell 2} p_T^{\nu 2} - \alpha^2)}}{E^{\ell 2} - p_z^{\ell 2}}, \quad (2.5)$$

where

$$\alpha = \frac{M_W^2}{2} + p_x^\ell p_x^\nu + p_y^\ell p_y^\nu. \quad (2.6)$$

If the discriminant of Eq.(2.5) is negative, which happens only if the actual momenta satisfy $(p^\ell + p^\nu)^2 > M_W^2$, it is reset to zero. The corresponding value of p_z^ν is adopted. This value of p_z^ν results in the smallest possible value for the mass of the $\ell\nu$ pair which is compatible with the known components of p^ℓ and p^ν . The corresponding mass is always larger than M_W . If the determinant is positive and the two solutions for p_z^ν have opposite sign we choose the solution whose sign coincides with that of p_z^ℓ . If they have the same sign we choose the solution with the smallest ΔR with the charged lepton. The reconstructed value is used for computing all physical observables.

All samples have been generated using CTEQ5L [20] parton distribution functions. For the $\mathcal{O}(\alpha_{EM}^6)$ and $\mathcal{O}(\alpha_{EM}^4 \alpha_S^2)$ samples, generated with PHANTOM, the QCD scale has been taken as

$$Q^2 = M_W^2 + p_{Ttop}^2 \quad (2.7)$$

if a triplet of final state particles with flavours compatible with deriving from the decay of a top or antitop quark can be found, while it has been taken as

$$Q^2 = M_W^2 + \frac{1}{6} \sum_{i=1}^6 p_{Ti}^2 \quad (2.8)$$

in all other cases. For the $\mathcal{O}(\alpha_{EM}^2 \alpha_S^4)$ sample the scale has been set to $Q^2 = M_Z^2$. This difference in the scales leads to a definite relative enhancement of the $4j + W$ background and of the MPI contribution compared to the other ones. Tests in comparable reactions have shown an increase of about a factor of 1.5 for the processes computed at $Q^2 = M_Z^2$ with respect to the same processes computed with the larger scale Eq.(2.8).

In our estimates below we have only taken into account the muon decay of the W boson. The $W \rightarrow e\nu$ channel gives the same result. The possibility of detecting high p_T taus has been extensively studied in connection with the discovery of a light Higgs in Vector Boson Fusion in the $\tau^+\tau^-$ channel [21] with extremely encouraging results. Efficiencies of order 50% have been obtained for the hadronic decays of the τ 's. The expected number of events in the $H \rightarrow \tau\tau \rightarrow e\mu + X$ is within a factor of two of the yield from $H \rightarrow WW^* \rightarrow e\mu + X$ for $M_H = 120$ GeV where the $\tau\tau$ and WW^* branching ratios of the Higgs boson are very close, suggesting that also in the leptonic decay channels of the taus the efficiency is quite high. Therefore we expect the $W \rightarrow \tau\nu$ channel to increase the detectability of the $Wjjjj$ final state.

3. MPI background to top pair production

The cross section for Single Particle Interaction processes and Multiple Parton Interactions contributing to the $jjjj(\mu^-\bar{\nu}_\mu + \mu^+\nu_\mu)$ final state, with the set of cuts in Eq.(2.3), are shown in the second column of Tab. 3. The cross sections in the third column have been obtained with the additional requirements:

$$\Delta R(jj) > 0.5 \quad \Delta R(jl^\pm) > 0.5 \quad (3.1)$$

which ensure that all jet pairs are well separated and that the charged lepton is isolated.

Process	Cross section	Cross section
$\mathcal{O}(\alpha_{EM}^4 \alpha_S^2)$	25.0 pb	22.0 pb
$\mathcal{O}(\alpha_{EM}^2 \alpha_S^4)$	64.7 pb	58.9 pb
$\mathcal{O}(\alpha_{EM}^2 \alpha_S^4)_{\text{DPI}}$	5.6 pb	5.3 pb
$\mathcal{O}(\alpha_{EM}^2 \alpha_S^4)_{\text{TPI}}$	0.27 pb	0.26 pb
$\mathcal{O}(\alpha_{EM}^6)$	0.22 pb	0.20 pb

Table 3: Cross sections for the processes which contribute to $4j + \ell\nu$. For the second column the selection cuts are given in Eq.(2.3). For the third column the additional requirements Eq.(3.1) have been applied.

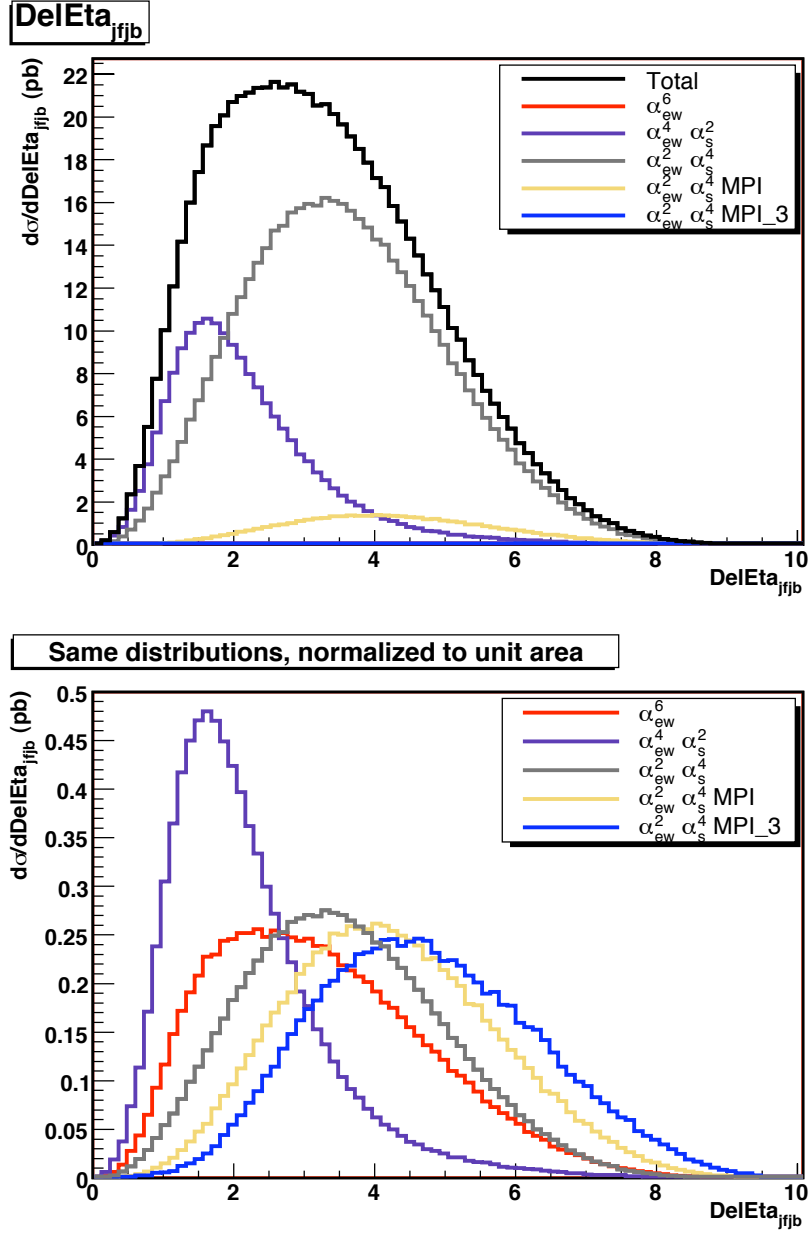


Figure 2:

$\Delta\eta$ separation between the most forward and most backward jet for the different contributions and for their sum. Cuts as in Eq.(2.3) and Eq.(3.1). The curves in the lower plot are normalized to one.

In Fig. 1 we show the invariant mass distribution of the triplet of jets with the highest combined transverse momentum which is expected to provide a good measurement of the top mass in the early phase of LHC [23], when b -tagging might be unavailable. The cross sections for masses in the range $170 \text{ GeV} < M_{jjj} < 180 \text{ GeV}$ are presented in Tab. 3.

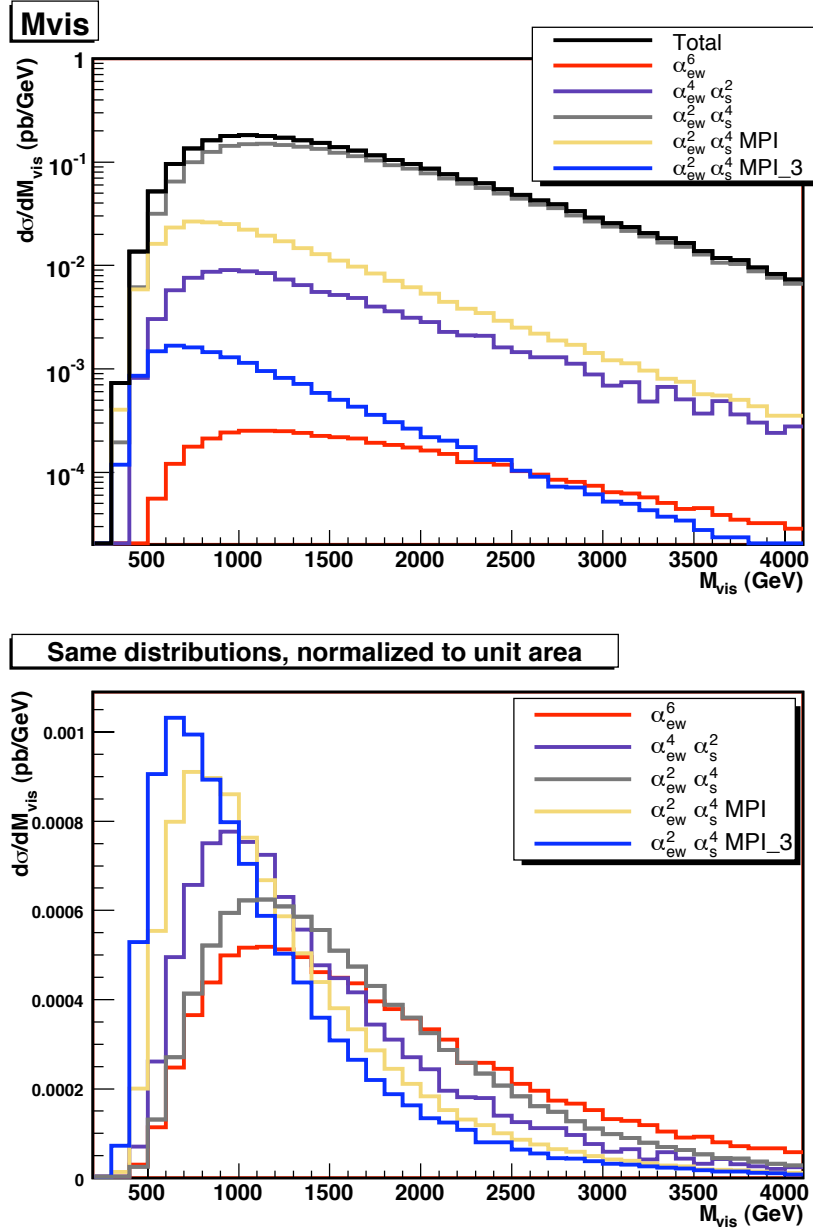


Figure 3: Visible mass distribution for the different contributions and for their sum. Cuts as in Eq.(2.3), Eq.(3.1) and Eq.(4.2). The curves in the lower plot are normalized to one.

This small mass interval has been selected purely for illustrational purposes. The actual smearing of the observed mass peak will be dominated by the uncertainty on the jet energy scale.

The $W + 4j$ $\mathcal{O}(\alpha_{EM}^2 \alpha_s^4)$ processes therefore provide a background of about 7% to top-antitop production in the semileptonic channel, while MPI processes provide a 1% background in this mass range. While such an increase of the background is unlikely to

Process	Cross section
$\mathcal{O}(\alpha_{EM}^4 \alpha_S^2)$	10.8 pb
$\mathcal{O}(\alpha_{EM}^2 \alpha_S^4)$	0.76 pb
$\mathcal{O}(\alpha_{EM}^2 \alpha_S^4)_{\text{DPI}}$	0.12 pb
$\mathcal{O}(\alpha_{EM}^2 \alpha_S^4)_{\text{TPI}}$	0.01 pb
$\mathcal{O}(\alpha_{EM}^6)$	0.04 pb

Table 4: Total cross sections in the mass range $170 \text{ GeV} < M_{jjj} < 180 \text{ GeV}$. Cuts as in Eq.(2.3) and Eq.(3.1).

affect the mass measurement, it might be relevant for the measurement of the cross section for $t\bar{t}$ production whose uncertainty is dominated by the background normalization [24].

It is obvious from the results in Tab. 3, that once b -tagging will be fully operational both the $W + 4j$ background and the MPI background will be completely negligible since only a very small fraction of events in these two samples contain b quarks while two b 's are always present in $t\bar{t}$ events.

4. Studying MPI in $W + 4j$ processes

Any attempt to detect MPI processes in the $jj(\mu^- \bar{\nu}_\mu + \mu^+ \nu_\mu)$ channel requires a strong suppression of top-antitop production. For this purpose, we have required that no jet triplet satisfies

$$|M_{jjj} - M_t| < 10 \text{ GeV} \quad (4.1)$$

Fig. 2 shows that MPI events tend to have larger separation in pseudorapidity between the most forward and most backward jets than $W + 4j$ or $t\bar{t}$ production. Therefore we require:

$$|\Delta\eta(j_f j_b)| > 3.8 \quad (4.2)$$

In a more realistic environment in which additional jets generated by showering cannot be ignored, one could impose condition (4.1) and (4.2) on the four most energetic jets in the event. The cross sections obtained after vetoing top production Eq.(4.1) and with the set of cuts in Eq.(2.3), Eq.(3.1) and Eq.(4.2) are shown in Tab. 5. Assuming a luminosity of 100 pb^{-1} this corresponds to a statistical significance of the MPI signal of about 6.1 if we take into account both the DPI and TPI contributions, and of 5.8 if we conservatively consider only DPI processes.

Fig. 3 presents the distribution on the invariant mass of the four jet plus charged lepton system. It shows that typically MPI events are less energetic than all other contributions considered in this paper.

In Fig. 4 we present the distribution of the largest $\Delta\phi$ separation between all jet pairs. Fig. 4 confirms that MPI processes leading to $W + 4j$ events are characterized by the presence of two jets which are back to back in the transverse plane. The $W + 4j$

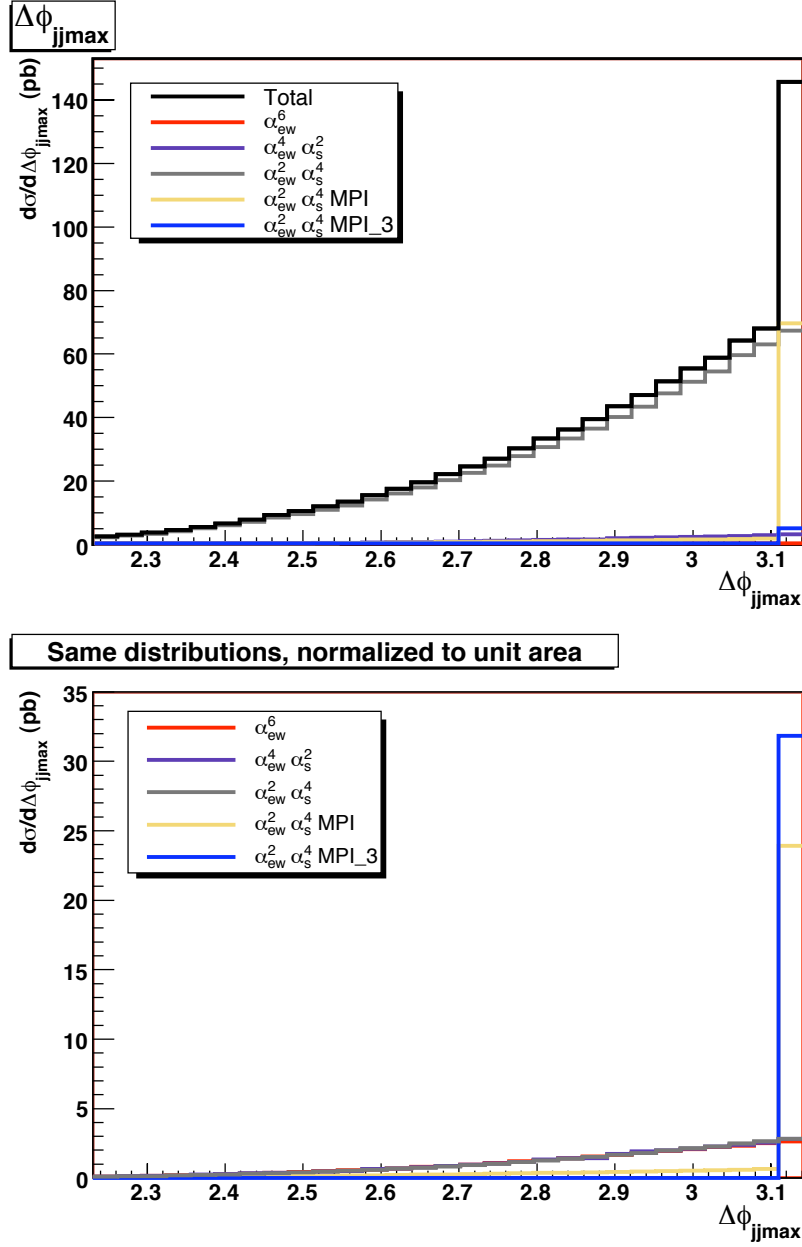


Figure 4: Largest $\Delta\phi$ separation between jet pairs for the different contributions and for their sum. Cuts as in Eq.(2.3), Eq.(3.1) and Eq.(4.2). The curves in the lower plot are normalized to one.

$\mathcal{O}(\alpha_{EM}^2 \alpha_S^4)$ contribution displays a much milder increase in the back to back region. All other contributions are negligible.

The expected $\Delta\phi$ resolution is of the order of a few degrees for both ATLAS [25] and CMS [26] for jets with transverse energy above 50 GeV. This resolution is comparable to the width of the bins in Fig. 4. We have examined the $\Delta\phi$ separation among pairs of jets

Process	Cross section
$\mathcal{O}(\alpha_{EM}^4 \alpha_S^2)$	1.16 pb
$\mathcal{O}(\alpha_{EM}^2 \alpha_S^4)$	24.01 pb
$\mathcal{O}(\alpha_{EM}^2 \alpha_S^4)_{\text{DPI}}$	2.91 pb
$\mathcal{O}(\alpha_{EM}^2 \alpha_S^4)_{\text{TPI}}$	0.16 pb
$\mathcal{O}(\alpha_{EM}^6)$	0.05 pb

Table 5: Total cross sections after vetoing the top, Eq.(4.1). Cuts as in Eq.(2.3), Eq.(3.1) and Eq.(4.2).

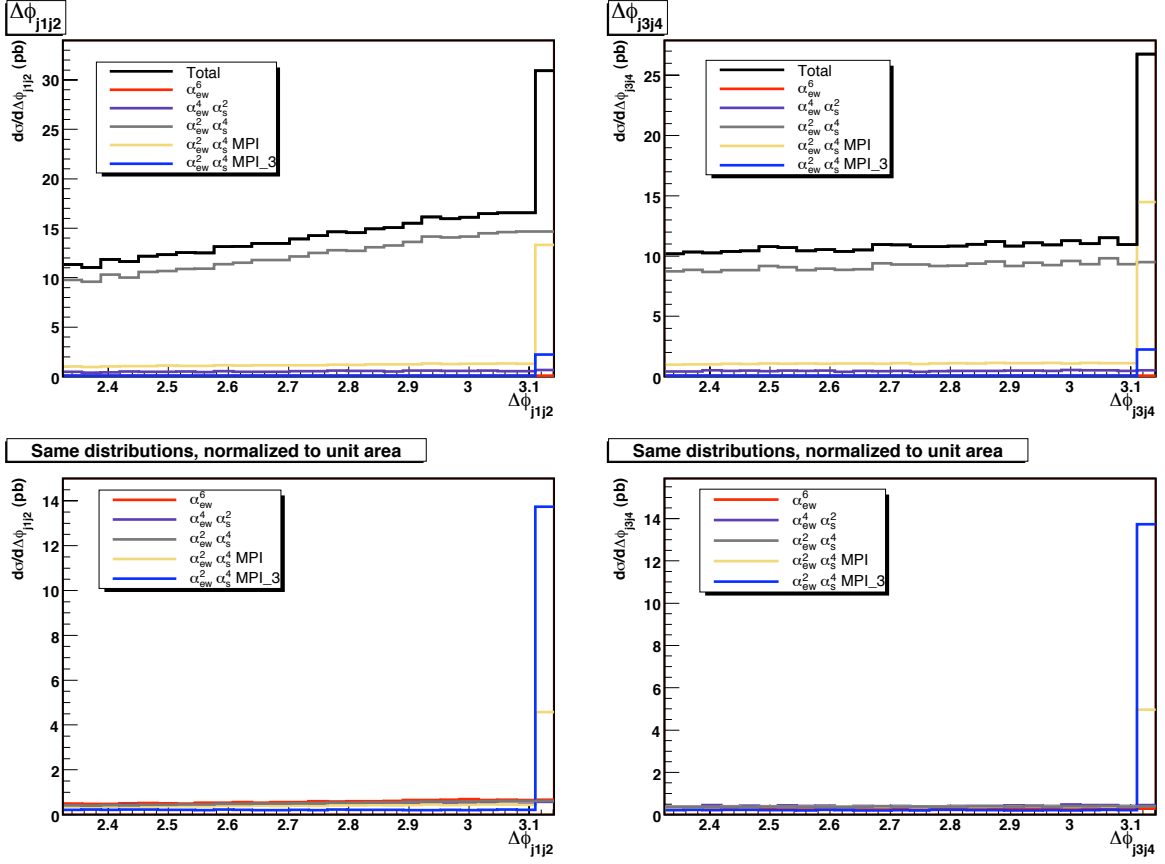


Figure 5: $\Delta\phi$ separation between the two most energetic jets (on the left) and between the two least energetic among the four jets (on the right) for the different contributions and for their sum. Cuts as in Eq.(2.3), Eq.(3.1) and Eq.(4.2). The curves in the lower plot are normalized to one.

ordered in energy, $E_{j_i} > E_{j_{i+1}}$. No clear pattern has emerged. In Fig. 5 we show the $\Delta\phi$ separation between the two most energetic jets, on the left, and of the two least energetic ones, on the right. As might have been guessed by the visible mass distribution in Fig. 3 the ratio between the MPI signal at $\Delta\phi = \pi$ and the $W + 4j$ background is somewhat

larger for softer jet pairs than for harder ones. It has proved impossible to clearly associate the two balancing jets with either the most forward/backward pair or with the central jets.

In conclusion, it appears quite feasible to achieve a good signal to background ratio, close to 1/1, for Multiple Interactions Processes compared to Single Interaction ones by selecting events with two jets with 180° separation in the transverse plane. It has not been possible to characterize further this pair of jets either through their energy or angular ordering.

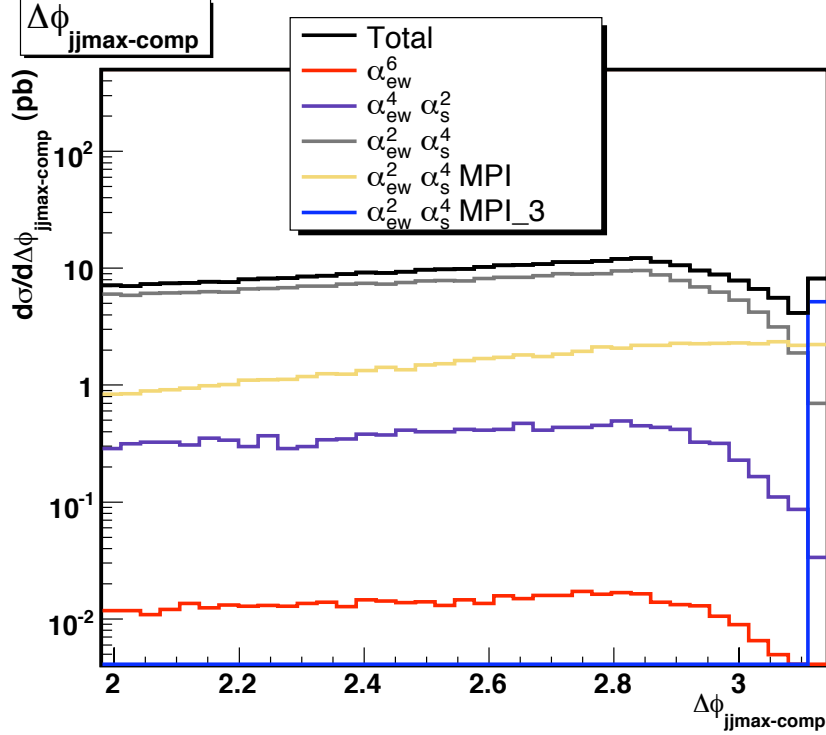


Figure 6: $\Delta\phi$ separation between the two jets which do not belong to the pair with the largest $\Delta\phi$ in the event. Cuts as in Eq.(2.3), Eq.(3.1), Eq.(4.2) and Eq.(4.3).

Let us now discuss Triple Parton Interactions in more detail. The obvious traits which characterize these events are the presence of two pairs of jets which balance in transverse momentum and of one W produced by a Drell-Yan interaction in which, to lowest order, the transverse momentum of the charged lepton is equal and opposite to the missing pT . While the first feature is not typically found in DPI, W bosons of Drell-Yan origin are present in $jjjj \otimes W$ events which account for about 15% of DPI. This is illustrated in Fig. 6 and Fig. 7. For these two plots we have only considered events in which the maximum $\Delta\phi$ among jets is in the interval:

$$|\Delta\phi(jj)_{max}| > 0.9 \cdot \pi \quad (4.3)$$

The corresponding cross sections are shown in Tab. 6. The rate decrease is of the order of 30% for Single Parton Interactions and essentially negligible for MPI processes. The

corresponding rates at the LHC are sizable. Even at low luminosity, $L = 30 \text{ fb}^{-1}$, about 5000 TPI events per year are expected.

Process	Cross section
$\mathcal{O}(\alpha_{EM}^4 \alpha_S^2)$	0.75 pb
$\mathcal{O}(\alpha_{EM}^2 \alpha_S^4)$	15.61 pb
$\mathcal{O}(\alpha_{EM}^2 \alpha_S^4)_{\text{DPI}}$	2.61 pb
$\mathcal{O}(\alpha_{EM}^2 \alpha_S^4)_{\text{TPI}}$	0.16 pb
$\mathcal{O}(\alpha_{EM}^6)$	0.03 pb

Table 6: Total cross sections with selection cuts in Eqs. 2.3, 3.1, 4.1, 4.2 and 4.3.

Fig. 6 shows the angular separation in the transverse plane between the two jets which do not belong to the pair with the largest $\Delta\phi$ in the event. The TPI contribution is concentrated at 180° while all other distributions are rather flat in that region. With the normalization $\sigma'_{eff} = \sigma_{eff}$ in Eq.(2.2), TPI give the largest contribution in the bin at $\Delta\phi = \pi$, amounting to more than 50% of the total.

Fig. 7 suggests that the presence of a charged lepton whose transverse momentum balances the missing pT is of limited use in separating TPI events from their background.

Because of the lack of information concerning the rate of Triple Parton Interactions, it is impossible to draw any firm conclusion from our preliminary analysis; Fig. 6 however suggests that indeed it might be possible to investigate TPI at the LHC exploiting the angular distribution of pairs of jets.

5. Conclusions

In this paper we have estimated for the first time the background provided by Multiple Parton Interactions to top-antitop production in the semileptonic channel at the LHC. We have concentrated on the early phase of data taking in which the mass will be measured from the invariant mass of jet triplets without resorting to b -tagging. The MPI background is about 1% in the mass region $M_{top} \pm 5 \text{ GeV}$, to be compared with a background of about 7% from $W + 4j$ via Single Parton Interactions.

The MPI contribution to $W + 4j$ is dominated by events with two jets with balancing transverse momentum. Both ATLAS and CMS have good resolution in the polar angle ϕ , and it looks possible to extract the MPI signal in this channel. Comparison with other reactions in which MPI processes can be measured should allow detailed studies of the flavour and fractional momentum dependence of Multiple Parton Interactions.

Our preliminary analysis suggests that it might be possible to investigate TPI at the LHC using the $jj \otimes jj \otimes W$ channel, which is the simplest process and the one with the largest rate which can give access to Triple Parton Interactions, exploiting the angular distribution of pairs of jets.

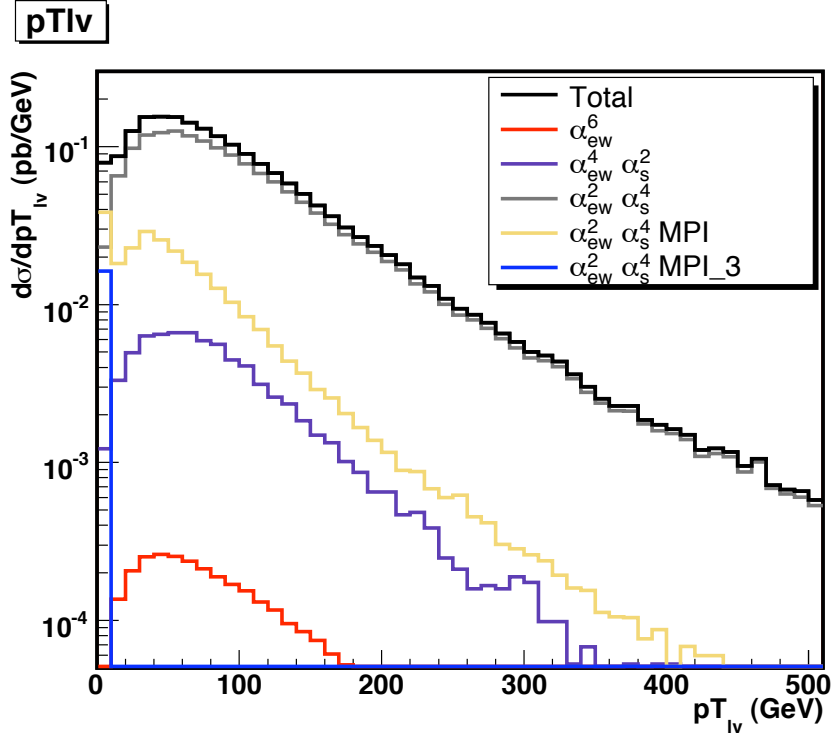


Figure 7: Distribution of the transverse momentum of the $l\nu$ system. Cuts as in Eq.(2.3), Eq.(3.1), Eq.(4.2) and Eq.(4.3).

Acknowledgments

We gratefully acknowledge several illuminating discussions with Roberto Chierici and Paolo Bartalini.

This work has been supported by MIUR under contract 2006020509_004 and by the European Community's Marie-Curie Research Training Network under contract MRTN-CT-2006-035505 'Tools and Precision Calculations for Physics Discoveries at Colliders'

References

- [1] T. Akesson *et al.* (Axial Field Spectrometer Collaboration), *Z. Phys.* **C34** (1987) 163.
- [2] F. Abe *et al.* (CDF Collaboration), *Phys. Rev. Lett.* **79** (1997) 584, F. Abe *et al.* (CDF Collaboration), *Phys. Rev.* **D56** (1997) 3811
- [3] A. Del Fabbro and D. Treleani, *Phys. Rev.* **D61** (2000) 077502, [hep-ph/9911358].
- [4] A. Del Fabbro and D. Treleani, *Phys. Rev.* **D66** (2002) 074012, [hep-ph/0207311].
- [5] M.Y. Hussein, *Nucl. Phys. Proc. Supp.* **B174**(2007)55, [hep-ph/0610207].
- [6] T. Sjöstrand and P.Z. Skands, *JHEP* **03** (2004) 053, [hep-ph/0402078].
- [7] T. Sjöstrand and P.Z. Skands, *Eur. Phys. J.* **C39** (2005) 129, [hep-ph/0408302].

- [8] J.M. Butterworth, J.R. Forshaw and M.H. Seymour, *Z. Phys.* **C72** (1996) 637, [hep-ph/9601371].
- [9] M. Bahr, S. Gieseke and M.H. Seymour, *JHEP* **07** (2008) 076, arXiv:0803.3633 [hep-ph].
- [10] A.M. Snigirev, *Phys. Rev.* **D68** (2003) 114012, [hep-ph/0304172].
- [11] V.L. Korotkikh and A.M. Snigirev, *Phys. Lett.* **B594** (2004) 171, [hep-ph/0404155].
- [12] E. Cattaruzza, A. Del Fabbro and D. Treleani, *Phys. Rev.* **D72** (2005) 034022, [hep-ph/0507052].
- [13] D. Treleani, *Phys. Rev.* **D76** (2007) 076006, arXiv:0708.2603 [hep-ph].
- [14] A. Ballestrero, A. Belhouari, G. Bevilacqua, V. Kashkan and E. Maina, arXiv:0801.3359 [hep-ph].
- [15] A. Ballestrero and E. Maina, *Phys. Lett.* **B350** (1995) 225, [hep-ph/9403244].
- [16] A. Ballestrero, PHACT 1.0 – *Program for Helicity Amplitudes Calculations with Tau matrices* [hep-ph/9911318] in *Proceedings of the 14th International Workshop on High Energy Physics and Quantum Field Theory (QFTHEP 99)*, B.B. Levchenko and V.I. Savrin eds. (SINP MSU Moscow), pg. 303.
- [17] F. Maltoni, T. Stelzer, *JHEP* 0302 (2003) 027; T. Stelzer and W. F. Long, *Comput. Phys. Commun.* **81** (1994) 357; J. Alwall *et al.*, arXiv:0706.2334; H. Murayama, I. Watanabe and K. Hagiwara, KEK-91-11.
- [18] J. Alwall *et al.*, A Standard format for Les Houches event files. Written within the framework of the MC4LHC-06 workshop: Monte Carlos for the LHC: A Workshop on the Tools for LHC Event Simulation (MC4LHC), Geneva, Switzerland, 17-16 Jul 2005, *Comp. Phys. Commun.* **176** (2007) 300, [hep-ph/0609017].
- [19] See for instance the recent talks by R. Field <http://www.phys.ufl.edu/~rfield/>
- [20] CTEQ Coll.(H.L. Lai *et al.*) *Eur. Phys. J.* **C12** (2000) 375.
- [21] S. Asai *et al.*, *Eur. Phys. J.* **C32 S2** (2004) 19.
- [22] C. Weiser, CERN-CMS-Note-2006-014.
- [23] F. Hubaut, hep-ex/0605029, Proceedings of 41st Rencontres de Moriond: QCD and Hadronic Interactions, La Thuile, Italy, 18-25 Mar 2006.
R. Chierici, CMS CR 2006/072, in Proceedings ICHEP 2006. Edited by A. Sissakian, G. Kozlov, E. Kolganova., Singapore, World Scientific, 2007.
- [24] M.Gosselink, arXiv:0810.3677 [hep-ex], Proceedings of 34th International Conference on High Energy Physics, Philadelphia, 2008.
- [25] ATLAS Collaboration, *Detector and Physics Performance Technical Design Report*, Vols. 1 and 2, CERN-LHCC-99-14 and CERN-LHCC-99-15.
- [26] CMS Collaboration, *Technical Design Report*, Vols. 1 and 2, CERN/LHCC 2006-001 and CERN/LHCC 2006-021.